Advanced Powder Technology 30 (2019) 1058–1066

Contents lists available at ScienceDirect

Advanced Powder Technology

journal homepage: www.elsevier.com/locate/apt

Original Research Paper

Effect of solvents on properties of the ultrasound assisted synthesized ceria nanoparticles and its performance as an adsorbent

Amruta Udaykumar Badnore [a,1], Ameya Pravin Chaudhari [b,1], Jay Kalpesh Patel [c,1], Aniruddha Bhalchandra Pandit [a,*]

[a] Department of Chemical Engineering, Institute of Chemical Technology, Matunga, Mumbai 400 019, India
[b] Department of Pharmaceutical Sciences and Technology, Institute of Chemical Technology, Matunga, Mumbai 400 019, India
[c] Department of Polymer Sciences and Engineering, Institute of Chemical Technology, Matunga, Mumbai 400 019, India

ARTICLE INFO

Article history:
Received 11 August 2018
Received in revised form 20 February 2019
Accepted 1 March 2019
Available online 12 March 2019

Keywords:
Ultrasound
Solvents
Zeta potential
Adsorption performance

ABSTRACT

The present study revealed a facile, ultrasound assisted ceria nanoparticle synthesis route by the reduction of cerium nitrate hexahydrate in different solvents at room temperature. The different solvents employed were methanol (MeOH), ethylene glycol (EG), water (aq) and isopropyl alcohol (IPA). The ceria nanoparticles were synthesized without the use of any capping agent in 20 min. The yield obtained was around 90% for the synthesized ceria samples. As synthesized ceria nanoparticles were characterized by X-ray diffraction (XRD), Field emission gun scanning electron microscopy (FEG-SEM), Brunauer Emmett Teller (BET) and zeta (ζ) potential in order to determine the influence of solvent on the physical properties of ceria nanoparticles. All the ceria samples illustrated a predominant spherical shape with the size in the range of 5–20 nm. It was found that interaction of the solvent with ceria nanoparticles in the presence of ultrasound plays an important role in modulating crystallite size, surface charge and its adsorption performance for a xylene milling yellow 6G dye. Among all the sonicated ceria samples, IPA mediated ceria exhibited highest positive zeta potential and hence was found to be proficient for the complete removal of dye in 15 min. Furthermore, the adsorption of the yellow milling dye on the surface of (IPA mediated) sonicated ceria sample has shown to follow pseudo-first order kinetic model. The non-sonicated sample (prepared in MeOH solvent without ultrasound) shows negligible dye adsorption while sonicated sample reveals 50% removal of XMY dye due to the difference in zeta potential values resulted from the cavitation effects.

1. Introduction

Ceria or Cerium Oxide (CeO_2) is a crystalline rare earth oxide and has attracted a lot of attention in the past few years owing its unique properties. The properties like ultraviolet radiation absorbing ability [1], high hardness index, high catalytic activity for reactions like wet air oxidation, reactivity and its stability at higher temperature allow it to have many applications [2]. Ceria has mainly been used in its nanoparticle form and has been developed for various applications such as glass polishing material [3], catalytic support or promoter [4], gas sensor [5], oxygen ion conductor in solid oxide fuel cells (SOFCs) [6], UV absorbent [1] and as an abrasive of the chemo-mechanical polishing slurry in semiconductor fabrication [7].

Ceria nanoparticles have been synthesized by several different methods, most popular being sonochemical [8,9], sol–gel process [10,11], solvothermal synthesis [12–16], forced hydrolysis [17], micro-emulsion [18], precipitation [19–22]. The sonochemical (acoustic cavitation) method of synthesis has been a very well-established method of nanoparticle synthesis for obtaining smaller and uniform particle size and high surface area [23]. This method is known to be simple to employ and cost effective on a lab scale. There are hotspots created through the adiabatic compressions or shockwave formation within the gas-vapour phase of the collapsing bubbles due to the implosion of the gas bubbles in acoustic cavitation [23,24]. The temperature inside the hotspot can reach up to ~5000 °C and the pressure can be >1800 atm [25]. Thus, ultrasonic

* Corresponding author at: Chemical Engineering Division, Institute of Chemical Technology, Matunga, Mumbai 400 019, India.
E-mail address: ab.pandit@ictmumbai.edu.in (A.B. Pandit).
[1] Co-first authors (equal contribution).

https://doi.org/10.1016/j.apt.2019.03.001
0921-8831/

waves in acoustic cavitation producing local high temperature and pressure spots, which aid in the formation of nanoparticles.

Some recent research articles have illustrated the ceria nanoparticle synthesis in different solvents. However, they have not studied the adsorption performance of the synthesized ceria nanostructures. Remani et al. have synthesized ceria nanoparticles in alcohol-water mixed solvents using ammonia and cerium nitrate hexahydrate as reactants via precipitation method [26]. Gu et al. have reported ceria (cerium oxide) nanoparticle synthesis by decomposing cerium oleate complex in different high boiling solvents [27]. From these previously reported works, it can be inferred that the choice of the solvent is important as the solvent properties such as polarity, viscosity, chain length, dielectric constant affects the synthesised nanoparticle physical characteristic. The milling yellow dye is an azo dye. The ceria nanoparticles are proved to be used for the adsorption of the azo dyes [28]. The electrostatic attraction between protonated hydroxyl surface of ceria and anionic dye ions of the dissociated sulphonate group promotes the adsorption of dye molecules.

In this report, ceria nanoparticles were synthesised at room temperature in different solvents viz. water, isopropyl alcohol, ethylene glycol and methanol using sonication assisted co-precipitation technique. A sample was synthesized in MeOH solvent without ultrasound but with a magnetic stirrer for the agitation. The yield of the synthesized ceria samples was evaluated. To the best of our knowledge, this is the first attempt to synthesize ceria nanoparticles in different solvents using sonication technique to explore the physical properties as well its adsorption efficacy. Furthermore, the kinetics of xylene milling yellow 6G dye adsorption on ceria nanoparticles (synthesized in solvent with suitable properties) has been studied.

2. Materials and methods

2.1. Materials

Cerium nitrate hexahydrate (99% purity) was obtained from S. D. Fine Chemicals Ltd., Mumbai, India. Sodium hydroxide (97.5% purity) and the HPLC grade solvents- deionized water (DI water), ethylene glycol (EG), methanol (MeOH) and isopropyl alcohol (IPA) were obtained from Thomas Baker Chemicals Pvt. Ltd., Mumbai, India. Xylene milling yellow 6G dye (98% purity) was purchased from Bombay Chemicals, India.

Ultrasound set up

A horn type ultrasound equipment was used for synthesis of ceria nanoparticles. The specifications of the equipment are given below.

Make: Dakshin India Ltd, Mumbai.

Operating frequency: 20 KHz, Diameter of stainless steel tip of horn: 0.019 m and Surface area of ultrasound irradiating face: 2.83×10^{-4} m^2.

Energy provided during sonochemical synthesis method (US)

- Actual efficiency of horn when it was operated for 7.5 min on cycle (irradiation time) calculated by calorimetric method = $m.C_p.dT$
  = 64.58 g × 4.18 J/g °C×(43–29)°C = 3779.2 J
- Theoretical efficiency of horn = Rated horn power × Irradiation time of horn i.e.7.5 min
  = 340 × 7.5 min × 60 s = 153,000 J
- Efficiency of horn = Actual η/Theoretical η
  = 3779.2 J/153,000 J = 2.47%

2.2. Synthesis of ceria nanoparticles

Below is the reaction scheme for the ceria nanoparticle synthesis. It is an instantaneous and co-precipitation type of reaction.

$$2Ce(NO_3)_3 \cdot 6H_2O + 6NaOH \rightarrow 2CeO_2 + 6NaNO_3 + 9H_2O$$

Cerium nitrate hexahydrate, 7.65 g (17.44 mmol) was dissolved in 60 ml of deionised water and sodium hydroxide, 2.14 g (52.166 mmol) was dissolved in 40 ml of deionised water separately with the aid of a water bath at 70 °C. The solutions were allowed to cool naturally. The sodium hydroxide solution was then added dropwise to the cerium nitrate hexahydrate solution under sonication at 20 KHz frequency with 1 s pulse and 1 s relaxation cycle from time t = 0 min (from start of addition) over 22 min. The time taken for the complete addition of sodium hydroxide solution to cerium nitrate hexahydrate solution was 22 min. The addition time was decided based on mixing time experiment described in our earlier work [29]. The mixture (sodium hydroxide and cerium nitrate hexahydrate solution) was further irradiated for 18 more min under same sonication parameters as that were used during the addition of sodium hydroxide solution to the cerium nitrate hexahydrate solution. Further irradiation time was fixed based on the maximum yield obtained. Similarly, Pinjari et al. have optimized the time required for ceria synthesis process based on the yield obtained and have reported that 18 more mins were required for the maximum ceria yield. It was for their experimental set-up, which was similar to that described in this work [30]. Different solvents viz. ethylene glycol (EG), methanol (MeOH) and isopropanol (IPA) were employed instead of water in order to study the influence of solvent on the yield, surface and structural as well as adsorption properties of CeO_2 NPs. All reactions were carried out at room temperature i.e. 27 ± 2 °C. But there was rise in temperature of the reaction mixture. The rise in temperature was around 10 °C after 20 min of ultrasound irradiation due to the hot spots generated during cavitation.

After the sonication the solution containing ceria nanoparticles was centrifuged using Tarsons 250 ml tubes with Eltek Centrifuge RC 4100F, being set at 7000 rpm (8052.95*g*) rotating speed and for 15 min of operating time. Supernatant was decanted while bottom yellow residue containing ceria nanoparticles was reslurried in deionised water using an ultrasonic horn for 4 min to ensure that the ceria nanoparticles were dispersed completely before the next stage of centrifugation. In the second phase of centrifugation, the reslurried yellow solution was centrifuged at 7000 rpm (8052.95*g*) for 30 min. Again, the obtained ceria nanoparticles were reslurried and washing process was repeated to remove the traces of solvent used during the reaction and the by-product, sodium nitrate before the third centrifugation. Finally, after third centrifugation, the collected ceria nanoparticles were redispersed in small amount of methanol for drying. When methanol gets evaporated the nanoparticles were oven dried at 100 °C for 48 h. Thereafter the dried ceria nanoparticles were weighed, crushed with a mortar and pestle and stored in a desiccator for analysis.

A single experiment was conducted to synthesize ceria in methanol solvent without the use of horn, using same concentration of reactants and conditions as that used in above described ultrasound irradiation method. The horn was replaced with a magnetic stirrer for the agitation and the sample synthesized is termed as non-sonicated ceria sample.

2.3. Adsorption experiments to study adsorption performance of the synthesized ceria nanoparticles

In order to test dye adsorption performance of the synthesized ceria nanoparticles, adsorption experiment was carried as follows:

In a typical adsorption experiment, 50 mg/L concentration of dye solution was prepared in a deionised water. The prepared dye solution (50 ml) was taken into a 100 ml beaker and the beaker was kept on a magnetic stirrer at an agitation speed of 500 rpm. 0.1 g of the synthesized ceria nanoparticles were added to the beaker containing the dye solution. An aliquot (2 ml) of the dye solution was pipetted out after every 5 min and was centrifuged (Lab Quest MCF08 VT centrifugation machine) at 6000 rpm (1854.72*g*) for 10 min. The absorbance of the obtained supernatant was checked by the UV spectrophotometer (Shimadzu UV-1800) in scan range of 200–500 nm wavelength. Each time, 1 ml supernatant sample was diluted with 1 ml of deionised water into the cuvette and the absorbance was measured. Similar procedure was repeated for each synthesized ceria nanoparticle to study and compare the adsorption rate of the dye on the nanoparticles. All the experiments were performed at room temperature.

To quantify and separate the solvent interaction and cavitation effect, an experiment was performed for the adsorption of XMY dye on non-sonicated ceria sample.

2.4. Experimental procedure to determine adsorption capacity and kinetics of XMY dye adsorption on ceria sample (synthesized in isopropyl solvent)

To know the adsorption capacity of the ceria nanoparticles (synthesized in IPA solvent), a dye solution of 100 mg/L concentration was made. 50 ml of the prepared dye solution was taken into a beaker and the beaker was kept on a magnetic stirrer with an agitation speed of 500 rpm. Synthesized ceria nanoparticles (0.02 g) were added to the beaker containing known concentration (100 mg/L) of dye solution and the samples were taken out at regular intervals to check their absorbance values after the separation of the suspended ceria nanoparticles by centrifugation. Absorbance of the aliquots was checked with the similar method described in Section 2.3. Experiments were carried out at room temperature.

To predict the adsorption kinetics of the dye on CeO_2 NPs (synthesized in IPA solvent), initial dye concentration of 100 mg/L and an amount of 0.1 g ceria was chosen.

3. Characterization

The ceria nanoparticles were characterized by X-Ray diffractometer (Bruker D8 advance, Germany) equipped with Cu Ka (λ = 1.54 Å) radiation source. The scan range of secondary monochromator was 10–80° (2θ-scale). The step of 0.02° per 0.2 s was given during the scan. The surface morphology and the particle size of ceria samples were estimated by JEOL JSM-7600F Field emission gun-scanning electron microscope (FEG-SEM) instrument. BET (Brunauer Emmett Teller) analysis was carried out on Smart Sorb 92/93 BET surface area analyser to estimate the surface area of the synthesized nanoparticles. The zeta (ζ) potential and hydrodynamic particle size of the synthesized ceria samples were investigated using NanoPlusAnalyzer, Germany.

4. Results and discussion

4.1. Yield and reaction time

Pinjari et al. reported that the time required for sonochemical synthesis of ceria nanoparticle was 20 min as against 4 h time required for conventional method of ceria synthesis [30]. Furthermore, they have evaluated and inferred that sonochemical method is energy efficient over conventional method of ceria synthesis as it saved more than 92% process energy. In this study, similar observation for reaction time have been found as that inferred by Pinjari et al. The time required for the complete conversion of reactants to form product (ceria) was found to be 20 min. Table 1 shows the yield assessed for the sonochemically synthesized ceria nanoparticles in different solvents. In all solvents, the yield obtained was in the range of 85–90% (Table 1) for 20 min reaction time. The percentage yield of ceria nanoparticle was calculated by taking the ratio of the measured final weight (average) of the ceria product after drying (after separating the by-products) to the stoichiometrically expected weight of product (ceria).

4.2. XRD analysis

Fig. 1 depicts X-ray diffraction pattern of ceria nanoparticles synthesized in different (IPA, EG, H_2O and MeOH) solvents using sonication method. XRD patterns were investigated to confirm product purity and to determine the crystallite size and phase of the synthesized CeO_2 NPs.

All the diffractograms (Fig. 1) displays nine peaks and are in good agreement with JCPDS card No. 34-0394 for ceria. 2 Theta values of all the ceria samples (as shown in Fig. 1.) well matches with each other. No additional peak was observed in the diffractograms in the Fig. 1 which indicates that the pure phase of ceria was formed. As per the JCPDS data, the observed nine peaks at 2θ in the XRD spectra can be indexed to face-centered cubic structure of crystalline ceria formed. All the peaks (Fig. 1) show broadening and is ascribed to the formation of ceria nanocrystals in ultrasound assisted solvent mediated synthesis technique. Debye scherrer formula was used to determine crystallite size of the ceria samples considering highest intensity peak position of 28.29°. Crystallite size values are displayed in Table 1. Debye scherrer formula is expressed as $D = K.\ \lambda/\beta \cdot \cos\theta$ and our previous work describes the terms in the given formula [29].

The crystallite size of ceria sample increases (Table 1) with an increase in the boiling point of the solvents. The crystallite size of ceria was found to be lowest in MeOH (4.37 nm) as compared to that obtained in other three solvents viz. IPA, EG and H_2O (illustrated in Table 1). This can be attributed to the lower boiling point of the MeOH. The lower is the boiling point of the solvent, higher is the vapour pressure which causes cavitation to be less effective i.e. it lowers collapse intensity of bubbles as the vapour enters the bubbles formed. Also lower the boiling point of solvent, lower it is heated owing to which it interacts less with the ultrasound waves [31,32]. It (less solvent interaction with ultrasound waves) causes methoxy groups of the solvent (methanol) to get locations majorly on the ceria surfaces preventing crystal growth of nanoparticles. This will envisage the crystallite size of CeO_2 NPs to be smaller. The crystallite size of ceria was found to highest (7.60 nm) in EG solvent. This is owing to low vapor pressure of the EG solvent due to which cavitation events are more intense though fewer in number and hence more effective locally. This is because at low vapor pressure of fluid, the bubbles are less occupied with the solvent vapours so the collapse of the bubbles are more violent. The increased diffusion and microstreaming during cavitation promote the migration of most of the solvent molecules away from ceria surfaces. This allows ceria crystals to get orientation at specific location which facilitates growth of the crystals resulting into higher crystallite size.

The % crystallinity of ceria samples were computed by the method described in our earlier work [29]. From the Table 2 it can be inferred that for all the ceria samples, the % crystallinity computed was found to be consistent with the crystallite size values. Hence the % crystallinity of ceria synthesized in EG solvent was observed to be highest (15.77%) while that synthesized in MeOH solvent was found to be lowest (9.04%). These results are in accordance with data observed for the synthesized ZnO NPs

Table 1
%Yield, crystallite size and % crystallinity of ceria nanoparticles synthesized in different solvents.

Solvents	Average weight (g)	%Yield (3 g basis)	Crystallite size (nm)	% Crystallinity
Ethylene glycol	2.648	88.27	7.60	15.77
Methanol	2.672	89.06	4.37	9.04
Water	2.606	86.86	7.22	14.93
Isopropyl alcohol	2.590	86.33	6.98	14.43

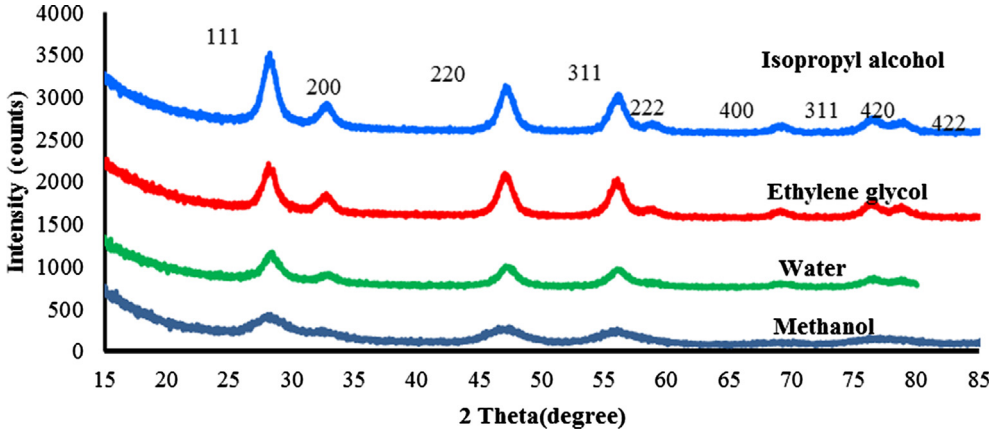

Fig. 1. XRD pattern of ceria nanoparticles synthesized by sonication method in different solvents: isopropyl alcohol, ethylene glycol, water and methanol.

Table 2
Particle size and surface area of ceria samples synthesized in different solvents.

Solvents	Average particle size estimated from Field emission gun scanning electron microscopy (FEG-SEM) (nm)	Particle size distribution assessed from Dynamic light scattering (DLS) method (nm)	Surface area (m^2/g)
Ethylene glycol	19.4	335.2-381	131.04
Methanol	9.89	302.3-255.4	155.77
Water	18.09	356.7-306.3	98.83
Isopropyl alcohol	17.9	333.4-270.8	113.47

(in our previous work) where % crystallinity was found to reduce due to a reduction in crystallite size [29].

4.3. FEG-SEM analysis

Fig. 2 demonstrates the FEG-SEM micrographs of as synthesized ceria nanoparticles in solvents viz. ethylene glycol, methanol, water and isopropyl alcohol using sonication method. The effect of solvents on the structure of ceria samples were investigated by FEG-SEM analysis. All the FEG-SEM micrographs shown in Fig. 2 are at a magnification of 100,000×. All the FEG-SEM micrographs illustrates predominant spherical shape of ceria nanoparticles. The particle size was calculated from SEM images by considering the population of 50 particles of a sample and averaging their size. The scale given in the FEG-SEM images was used to assess the size of the particles. The lower boiling point ensued smaller particles while higher boiling point will lead to higher size of nuclei formation under cavitation conditions as mentioned earlier in Section 4.2. The atomic size decides the crystallite size while the particle size is the aggregation of a number of atoms. So, the particle size of the samples is greater than their crystallite size values (Tables 1 and 2). The particle size of ceria nanoparticles follows same kind of order of increase as those yielded for the crystallite size values, evidenced in Table 2. The average particle size measured from FEG-SEM images for all the ceria samples are in good agreement with the particle size distribution observed. The particle size distribution of ceria samples obtained by dynamic light scattering (DLS) method are illustrated in Table 2. The obtained particle size distribution for MeOH mediated ceria sample was found to be narrower as compared to the other three ceria samples. The reason being the confinement of nuclei formed during the CeO_2 NPs synthesis in lower boiling point solvent causing generation of smaller particles. In all four solvents, the particle size of CeO_2 NPs are in the range of 5–20 nm (Fig. 2). The smallest size of ceria was obtained in methanol solvent and the average particle size is estimated to be 9.89 nm (Table 2).

4.4. BET analysis

The textural properties of the as synthesized ceria samples (adsorbent) were analysed by BET analyser. The measured surface area of the synthesized ceria samples is shown in Table 2. Samples were degassed prior to the analysis at 100 °C for 2 h. There is physical adsorption of nitrogen gas on the solid surface of the samples at liquid nitrogen temperature of −196.15 °C. At 0.970 relative pressure (P/P_0) which is used to assess their surface area. The surface area was determined by single point measurement method.

The smaller size of nanoparticles provides higher surface area. Hence, ceria sample synthesized in methanol solvent possess highest surface area (Table 2) as compared to the samples synthesized in other solvents (EG, IPA and H_2O). The measured surface area of ceria samples is consistent with the crystallite size examined

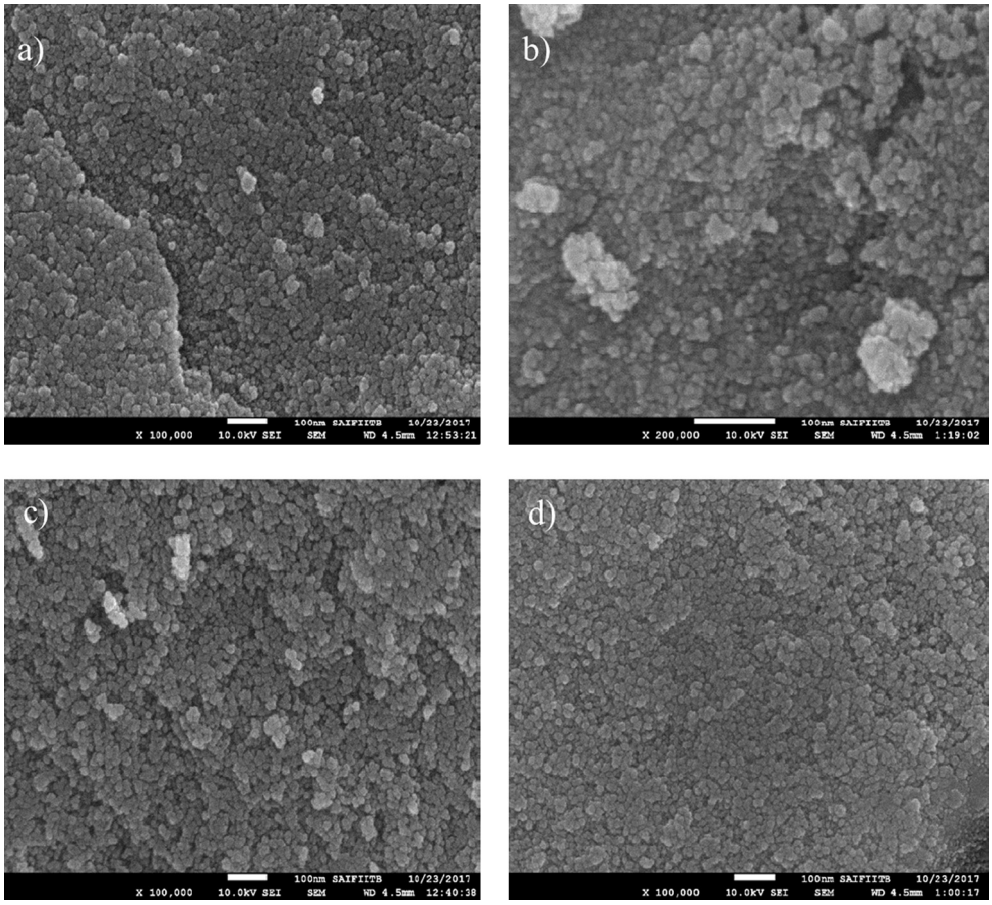

Fig. 2. FEG-SEM images of ceria nanoparticles synthesized in (a) ethylene glycol, (b) methanol, (c) water and (d) isopropyl alcohol using sonication method at room temperature.

(Table 2) except CeO_2 NPs synthesized in EG solvent. This can be attributed to the diol functional group of ethylene glycol which not only acts as a solvent but also as a surfactant during ceria synthesis. This forms the uniform spherical structure of ceria nanoparticles consequently increasing its surface area. A similar outcome of structure uniformity was inferred from the Hai et al. study [33]. They observed that the ethylene glycol acts as a surfactant as well as the solvent for improving the size uniformity of the magnesium oxide nanoparticles. Further, solvent has also decreased the agglomeration degree of the formed MgO nanoparticles.

4.5. Zeta (ζ) potential

Zeta potential (surface charge) plays an imperative role in adsorption of dye molecule. It influences the rate of adsorption of dye. Zeta potential measurements of the synthesized CeO_2 NPs are elucidated in Table 3. Around 5 mg of each ceria sample was dispersed in 10 ml of deionised water by sonication in ultrasonic bath for 15 min. After dispersion of nanoparticles of ceria in water, ceria samples were subsequently analysed for zeta potential.

Table 3
Zeta potential of ceria nanoparticles synthesized in different solvents.

Solvent	Zeta potential (mV)
Ethylene glycol	19.19
Methanol	−3.09
Water	15.19
Isopropyl alcohol	37.74

The ceria nanoparticles synthesized in IPA solvent possess highest positive zeta potential (37.74 mV) as compared to the ceria samples synthesized in other solvents (Table 3). The zeta potential of the nanoparticles synthesized in isopropanol, water and ethylene glycol follow the polarity trend. IPA being the least polar has the highest zeta potential and water being the most polar has the lowest zeta potential. Methanol is an outlier due to the high adsorption of methoxy groups on the active sites. This could be due to the high acidity of methanol, due to which methanol can easily dissociate into methoxy group and get adsorbed on the nanoparticles [34]. The reason for the difference in zeta potential can be explained based on the polarity of the solvents used. IPA being the least polar as compared to other solvents (H_2O and EG), cannot dissociate easily to form H^+ and its conjugate base. As against this, water being more polar as compared to the solvents IPA and EG, will dissociate easily to interact with ceria surfaces thus reducing its zeta potential value.

So, the interaction of solvent species with ceria nanoparticles plays an important role in influencing the nature of zeta potential of synthesized ceria nanoparticles. Based on this, IPA mediated ceria sample could be best speculated to adsorb anionic dye species.

4.6. Adsorption efficiency of the synthesized ceria nanoparticles

The experimental method is described in Section 2.3 to check the adsorption performance of dye on the four different synthesized ceria nanoparticles. Fig. 3 elucidates maximum absorption of xylene milling yellow 6G (XMY) dye at 398.5 nm wavelength so the residual dye concentration is measured at 398.5 nm wavelength for further UV analysis.

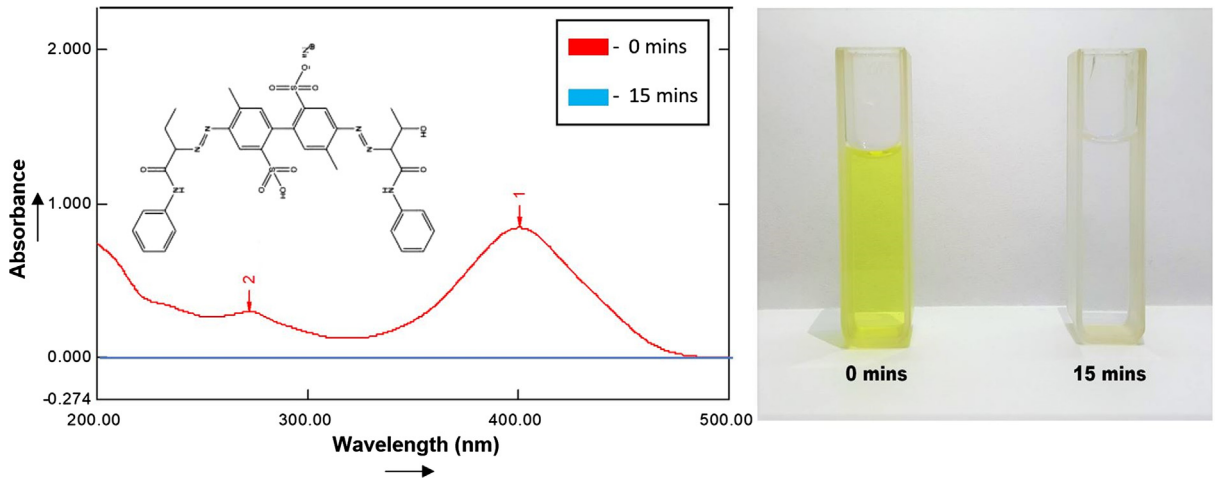

Fig. 3. Adsorption of xylene milling yellow dye by ceria nanoparticles (synthesized in IPA solvent). (For interpretation of the references to colour in this figure legend, the reader is referred to the web version of this article.)

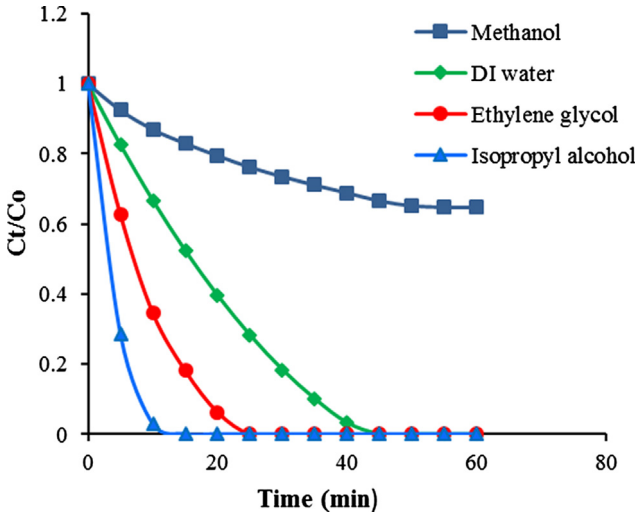

Fig. 4A. Comparative analysis of the adsorption rates displayed by the ceria nanoparticles synthesized in Methanol, DI Water, Ethylene glycol and Isopropyl alcohol.

Fig. 4A represent the adsorption performance of XMY dye on the surfaces of ceria nanoparticles fabricated in MeOH, DI H_2O, EG and IPA solvents. IPA mediated ceria sample showed (Fig. 4A) a remarkable effect on the rate of adsorption as the time taken for the complete removal of dye by CeO_2 NPs (synthesized in IPA solvent) was only 15 min. This can be attributed to the highest zeta potential (ζ = +37.74 mV) of CeO_2 NPs synthesized in IPA solvent as compared to the ceria nanoparticles synthesized into other solvent system (MeOH, DI H_2O and EG) as is evident from Table 3. This implies that the surface of CeO_2 NPs synthesized in IPA solvent are more positively charged as compared to the CeO_2 NPs synthesized into MeOH, DI H_2O and EG as a solvent. This leads to an electrostatic attraction of anionic species of XMY dye on the surface of CeO_2 NPs (synthesized in IPA solvent).

For the EG and H_2O mediated synthesized ceria samples, the time taken for the complete removal of XMY anionic species was found to be 25 and 45 min respectively. The longest time (more than 60 mins) taken for complete removal of XMY dye species was observed for CeO_2 NPs synthesized in methanol solvent. This is attributed to the negative surface charge of the CeO_2 NPs which increases the magnitude of the repulsive force between XMY anionic species and negatively charged CeO_2 NPs. It could be inferred from the Fig. 4A, that the rate of dye adsorption is a function of zeta potential of the synthesized ceria nanoparticles.

The order of adsorption efficiency of the synthesized ceria nanoparticles in different solvents is shown below.

$$IPA > EG > H_2O > MeOH$$

This trend doesn't concur with the surface area trend observed in Table 2. This is because the dye is anionic, the surface charge plays a major role in determining the nanoparticle's adsorption

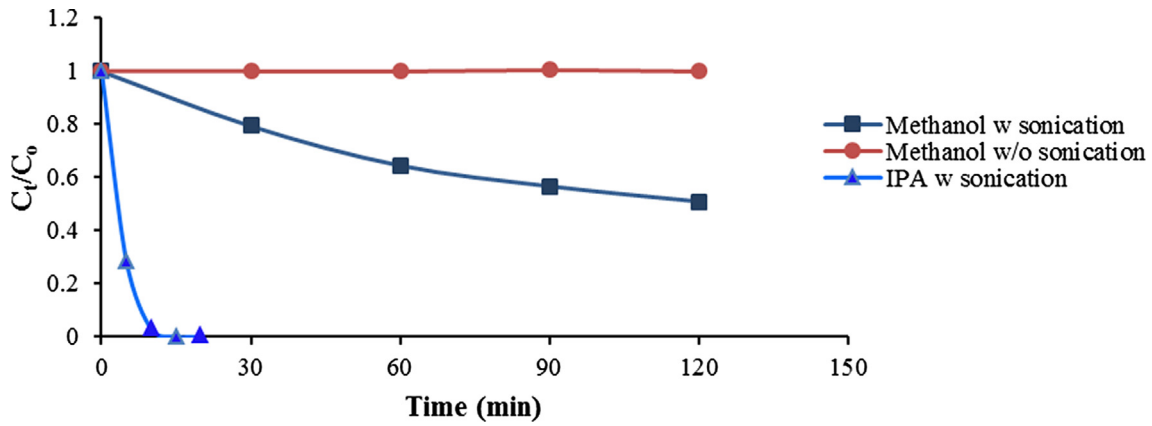

Fig. 4B. Comparative analysis of the adsorption rates displayed by the ceria nanoparticles synthesized in the methanol solvent with and without sonication method.

capacity. If it had not been any difference in the surface charge of ceria samples then the surface area would have contributed more to its physical adsorption efficiency than their zeta potential values.

Thus, it can be concluded that adsorption efficiency of ceria nanoparticles follows a similar trend as that observed for the zeta potential results (Table 3).

The non-sonicated and sonicated ceria sample, synthesized in methanol solvent were used to analyse and compare the adsorption rate of XMY dye on the synthesized ceria samples as depicted in Fig. 4B. Also, Fig. 4B demonstrates the adsorption rate of dye on the ceria synthesized in IPA solvent under sonication. It (ceria sample) has the highest zeta potential i.e. 37.74 mV and hence the highest anion adsorption efficiency.

Fig. 4B shows that the adsorption rate of dye on sonicated sample is much faster as compared to the dye adsorption rate on non-sonicated sample for methanol solvent. At 120 min, the non-sonicated sample shows negligible dye adsorption while sonicated sample reveals 50% removal of XMY dye (Fig. 4B). This is attributed to characteristics of cavitation in solvent medium. The cavitation induced during ceria synthesis in methanol solvent, preclude the interaction of methoxy group with ceria nanoparticle surface. As against this under the cavitation free condition, the solvent-nanoparticle interactions are promoted resulting into the zeta potential of −29.49 mV (ζ of sonicated sample = −3.09 mV) for the non-sonicated sample. This has extremely reduced the dye adsorption efficiency of non-sonicated sample. The shock waves generated during cavitation reduces the interaction of methoxy species with ceria surfaces. Thus, it can be inferred that cavitation plays a major role in altering the surface properties of the synthesized ceria nanoparticles.

4.7. Adsorption capacity

The adsorption capacity of ceria nanoparticles (synthesized in isopropyl solvent) was calculated as it gave the highest rate (Refer to the Fig. 4) of dye adsorption. The formula for calculating adsorption capacity is given below.

$$\text{Adsorption capacity}: \quad q_e = (C_o - C_e) \times V/W$$

where q_e is the amount of dye adsorbed at equilibrium time (mg/g), C_o is the initial concentration of dye (mg/L), C_e is the equilibrium concentration of dye after adsorption (mg/L), V is the volume of the dye solution (L) and W is the amount of ceria nanoparticle (g).

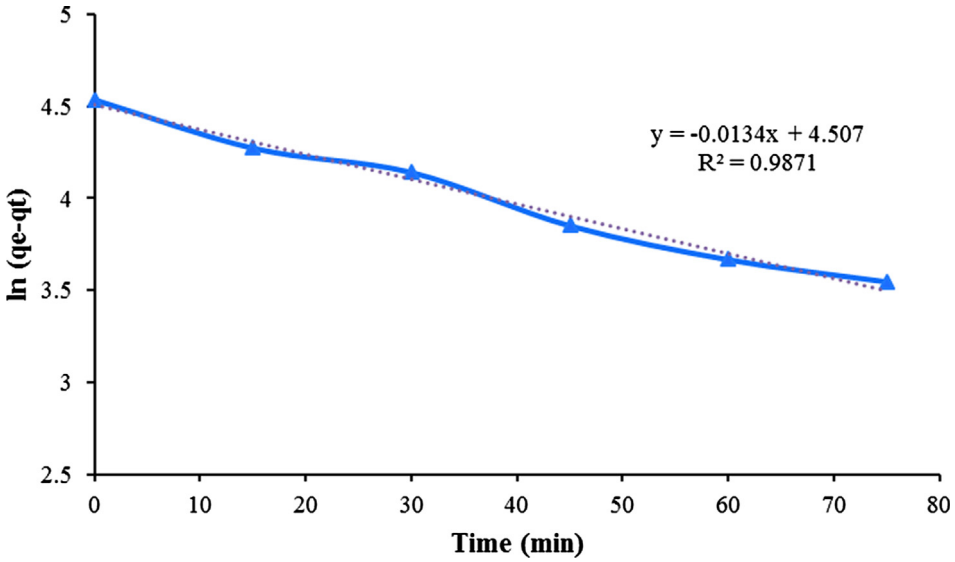

Fig. 5. Kinetics plot for XMY dye adsorption on CeO_2 NPs (synthesized in IPA solvent).

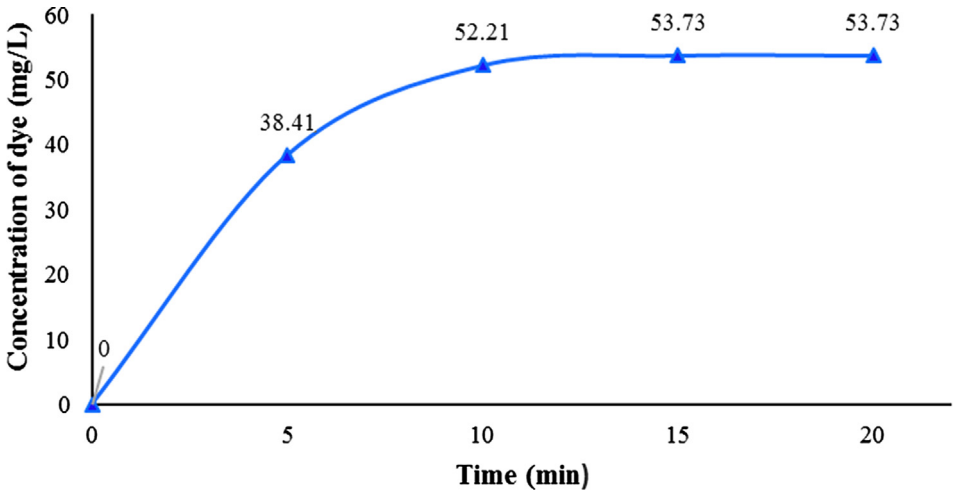

Fig. 6. Concentration of dye adsorbed on ceria (IPA mediated ceria sample) for initial dye concentration of 50 ppm and at 0.1 g of catalyst loading.

So, the adsorption capacity of ceria nanoparticle (synthesized in IPA solvent) was evaluated to be 93.354 mg/g for the specified experimental conditions mentioned in Section 2.4.

4.8. Kinetic study

Since the active sites of ceria nanoparticles were in excess (please refer supplementary information), the residual dye concentrations were measured initially and at particular time intervals. From this data the q_e and the q_t values were calculated.

where q_t = (Dye adsorbed × Vol. of beaker)/Amount of ceria used

= (Dye adsorbed × 50/1000)/0.02 g

and $q_e = q_t$ at equilibrium

The linearized form of the pseudo-first order equation [35] is:

$$\ln(q_e - q_t) = \ln q_e - k_1 \times t$$

The data obtained was analysed by allowing it to fit into the Lagergren's pseudo-first order kinetic model. From Fig. 5 it can be inferred that adsorption data satisfies well pseudo-first order kinetic model expression with rate dependency on dye concentration. The experimental data obeys pseudo-first order kinetics. The resultant plot has good correlation coefficient (R^2) value of 0.98. Hence the adsorption of yellow milling dye on the surface of (IPA mediated) synthesized ceria nanoparticles has been proposed to follow pseudo-first order kinetic model.

Fig. 6 illustrates the graph of the concentration of dye adsorbed (mg/L) on IPA mediated ceria sample versus time (min). From the nature of the graph, we can predict that the dye diffusion through the surface boundary of the ceria particles and attains equilibrium. Further, the nature of the plot obtained shows that the dye does not diffuse into the pores of the ceria sample hence pseudo second order and intraparticle diffusion does not have a significant role in the adsorption process.

5. Conclusions

Ceria nanoparticles were successfully synthesized in different solvents like methanol, water, isopropyl alcohol and ethylene glycol at room temperature using sonication method in 20 min. The technique was fast, simple and energy efficient to account around 90% yield of all the synthesized ceria samples. It was found that interaction of the solvent with ceria nanoparticles in the presence of ultrasound modulated the physical properties and adsorption efficiency of ceria for a xylene milling yellow 6G dye. The ultrasound-assisted ceria sample synthesized in isopropyl solvent showed highest positive zeta potential (+37.74 mV) and adsorption efficacy (complete removal of dye in 15 min) as compared to other three solvents (EG, H_2O and MeOH) used in this work. Hence solvent choice was inferred to be an important criterion in governing the rate of adsorption of dyes on ceria nanoparticles. The maximum adsorption capacity of IPA mediated ceria (sonicated) sample was found to be 93.35 mg of dye/g of ceria. Moreover, the adsorption of the yellow milling dye on the surface of synthesized ceria nanoparticles (IPA mediated) results reveal to have followed a pseudo-first order kinetic model. Under the cavitation free condition, the solvent-nanoparticle interactions are promoted resulting into the zeta potential of −29.49 mV (ζ of sonicated, methanol mediated sample = −3.09 mV) for the non-sonicated, methanol mediated ceria sample. The non-sonicated sample shows negligible dye adsorption while sonicated sample reveals 50% removal of XMY dye.

Acknowledgement

We are grateful to the UGC (University Grants Commission), India, for financial assistance and would also like thank UGC for providing a fellowship to one of the authors, AUB.

Appendix A. Supplementary material

Supplementary data to this article can be found online at https://doi.org/10.1016/j.apt.2019.03.001.

References

[1] S. Tsunekawa, R. Sahara, Y. Kawazoe, A. Kasuya, Origin of the blue shift in ultraviolet absorption spectra of nanocrystalline CeO_2−x particles, Mater. Trans., JIM 41 (2000) 1104–1107.
[2] A. Trovarelli, C. de Leitenburg, M. Boaro, G. Dolcetti, The utilization of ceria in industrial catalysis, Catal. Today 50 (1999) 353–367.
[3] S.-H. Lee, Z. Lu, S. Babu, E. Matijević, Chemical mechanical polishing of thermal oxide films using silica particles coated with ceria, J. Mater. Res. 17 (2002) 2744–2749.
[4] E. Bekyarova, P. Fornasiero, J. Kašpar, M. Graziani, CO oxidation on Pd/CeO_2–ZrO_2 catalysts, Catal. Today 45 (1998) 179–183.
[5] N. Izu, W. Shin, N. Murayama, S. Kanzaki, Resistive oxygen gas sensors based on CeO_2 fine powder prepared using mist pyrolysis, Sens. Actuators, B: Chem. 87 (2002) 95–98.
[6] H. Yahiro, Y. Baba, K. Eguchi, H. Arai, High temperature fuel cell with ceria-yttria solid electrolyte, J. Electrochem. Soc. 135 (1988) 2077–2080.
[7] M. Jiang, N.O. Wood, R. Komanduri, On the chemo-mechanical polishing (CMP) of Si_3N_4 bearing balls with water based CeO_2 slurry, J. Eng. Mater. Technol. 120 (1998) 304–312.
[8] K. Prasad, D. Pinjari, A. Pandit, S. Mhaske, Phase transformation of nanostructured titanium dioxide from anatase-to-rutile via combined ultrasound assisted sol–gel technique, Ultrason. Sonochem. 17 (2010) 409–415.
[9] K. Prasad, D. Pinjari, A. Pandit, S. Mhaske, Synthesis of titanium dioxide by ultrasound assisted sol–gel technique: effect of amplitude (power density) variation, Ultrason. Sonochem. 17 (2010) 697–703.
[10] X. Chu, W.I. Chung, L.D. Schmidt, Sintering of Sol—Gel prepared submicrometer particles studied by transmission electron microscopy, J. Am. Ceram. Soc. 76 (1993) 2115–2118.
[11] A. Makishima, H. Kubo, K. Wada, Y. Kitami, T. Shimohira, Yellow coatings produced on glasses and aluminum by the sol-gel process, J. Am. Ceram. Soc. 69 (1986).
[12] Y. Hakuta, S. Onai, H. Terayama, T. Adschiri, K. Arai, Production of ultra-fine ceria particles by hydrothermal synthesis under supercritical conditions, J. Mater. Sci. Lett. 17 (1998) 1211–1213.
[13] N.C. Wu, E.W. Shi, Y.Q. Zheng, W.J. Li, Effect of pH of medium on hydrothermal synthesis of nanocrystalline cerium (IV) oxide powders, J. Am. Ceram. Soc. 85 (2002) 2462–2468.
[14] M. Hirano, E. Kato, Hydrothermal synthesis of nanocrystalline cerium (IV) oxide powders, J. Am. Ceram. Soc. 82 (1999) 786–788.
[15] N. Uekawa, M. Ueta, Y.J. Wu, K. Kakegawa, Synthesis of CeO_2 spherical fine particles by homogeneous precipitation method with polyethylene glycol, Chem. Lett. 31 (2002) 854–855.
[16] E. Verdon, M. Devalette, G. Demazeau, Solvothermal synthesis of cerium dioxide microcrystallites: effect of the solvent, Mater. Lett. 25 (1995) 127–131.
[17] X. Dong, G. Hong, D. Yu, D. Yu, Synthesis and properties of cerium oxide nanometer powders by pyrolysis of amorphous citrate, J. Mater. Sci Technol. 13 (1997) 113–116.
[18] T. Masui, K. Fujiwara, K.-I. Machida, G.-Y. Adachi, T. Sakata, H. Mori, Characterization of cerium (IV) oxide ultrafine particles prepared using reversed micelles, Chem. Mater. 9 (1997) 2197–2204.
[19] X.-D. Zhou, W. Huebner, H.U. Anderson, Room-temperature homogeneous nucleation synthesis and thermal stability of nanometer single crystal CeO_2, Appl. Phys. Lett. 80 (2002) 3814–3816.
[20] B. Aiken, W.P. Hsu, E. Matijević, Preparation and properties of monodispersed colloidal particles of lanthanide compounds: III, yttrium (III) and mixed yttrium (III)/cerium (III) systems, J. Am. Ceram. Soc. 71 (1988) 845–853.
[21] P.L. Chen, I.W. Chen, Reactive cerium (IV) oxide powders by the homogeneous precipitation method, J. Am. Ceram. Soc. 76 (1993) 1577–1583.
[22] B. Djuričić, S. Pickering, Nanostructured cerium oxide: preparation and properties of weakly-agglomerated powders, J. Eur. Ceram. Soc. 19 (1999) 1925–1934.
[23] H. Xu, B.W. Zeiger, K.S. Suslick, Sonochemical synthesis of nanomaterials, Chem. Soc. Rev. 42 (2013) 2555–2567.
[24] V.S. Moholkar, S.P. Sable, A.B. Pandit, Mapping the cavitation intensity in an ultrasonic bath using the acoustic emission, AIChE J. 46 (2000) 684–694.
[25] A. Mahulkar, C. Riedel, P. Gogate, U. Neis, A. Pandit, Effect of dissolved gas on efficacy of sonochemical reactors for microbial cell disruption: experimental and numerical analysis, Ultrason. Sonochem. 16 (2009) 635–643.

[26] K.C. Remani, S. Ghosh, Nanocrystalline ceria through homogeneous precipitation in alcohol-water mixed solvent, Trans. Indian Ceram. Soc. 68 (2009) 185–188.
[27] H. Gu, M.D. Soucek, Preparation and characterization of monodisperse cerium oxide nanoparticles in hydrocarbon solvents, Chem. of Mater. 19 (2007) 1103–1110.
[28] N.M. Tomic, Z.D. Dohčević-Mitrović, N.M. Paunović, D.Z. Mijin, N.D. Radić, B.V. Grbić, S.M. Aškrabić, B.M. Babić, D.V. Bajuk-Bogdanović, Nanocrystalline $CeO_{2-\delta}$ as effective adsorbent of azo dyes, Langmuir 39 (2014) 11582–11590.
[29] A.U. Badnore, A.B. Pandit, Effect of pH on sonication assisted synthesis of ZnO nanostructures: process details, Chem. Eng. Process: Process Intensif. 122 (2017) 235–244.
[30] D.V. Pinjari, A.B. Pandit, Room temperature synthesis of crystalline CeO_2 nanopowder: advantage of sonochemical method over conventional method, Ultrason. Sonochem. 18 (2011) 1118–1123.
[31] P.B. Khoza, M.J. Moloto, L.M. Sikhwivhilu, The effect of solvents, acetone, water, and ethanol, on the morphological and optical properties of ZnO nanoparticles prepared by microwave, J. Nanotechnol. 2012 (2012).
[32] D. Peters, Ultrasound in materials chemistry, J. Mater. Chem. 6 (1996) 1605–1618.
[33] C. Hai, S. Li, Y. Zhou, J. Zeng, X. Ren, X. Li, Roles of ethylene glycol solvent and polymers in preparing uniformly distributed MgO nanoparticles, J. Asian Ceram. Soc. 5 (2017) 176–182.
[34] C. Yang, F. Bebensee, A. Nefedov, C. Wöll, T. Kropp, L. Komissarov, C. Penschke, R. Moerer, J. Paier, J. Sauer, Methanol adsorption on monocrystalline ceria surfaces, J. Catal. 336 (2016) 116–125.
[35] S.K. Lagergren, About the theory of so-called adsorption of soluble substances, Sven. Vetenskapsakad. Handingarl 24 (1898) 1–39.